

# Temporal Patterns of Individual Neuronal Firing in Rat Dorsal Column Nuclei Provide Information Required for Somatosensory Discrimination

Shin-ichiro Shishido<sup>1,2</sup> and Takashi Toda<sup>1</sup>

<sup>1</sup>Division of Oral Physiology, Tohoku University Graduate School of Dentistry, Sendai, Miyagi, Japan

<sup>2</sup>Akamori Oriental Medical College, Sendai, Miyagi, Japan

A wealth of mechanical information from the body generates various forms of sensory experience during touch or kinesthesia. Dorsal column nuclei (DCN) in the medulla are the first relay station for somatosensory inputs from peripheral receptors. These nuclei integrate somatosensory information and send the output to higher-order centers; therefore, investigating the firing patterns of DCN neurons should elucidate coding principles within the somatosensory system. In this study, we quantified the firing patterns of DCN neurons and examined whether the firing patterns of particular neurons are altered when moving tactile stimuli are applied in different directions. The activities of 17 neurons in the DCN of anesthetized rats were selected and their firing patterns were analyzed using LvR, which refers to the local variation of intervals of action potentials (*i.e.*, the cross-correlation between consecutive intervals of action potentials) compensated by the refractoriness constant, *R*. The LvR of the 17 neurons ranged widely from 0.35 to 2.28. Of the 17 neurons, 12 responded to hair deflection (hair neurons), whereas five responded specifically to movement of forelimb joints. In 11 of 12 hair neurons, moving stimuli were applied in two to four different directions, which yielded 25 pairs of comparisons. Of these, 14 pairs (56%) showed significant differences in LvR. Among these 14 pairs, the range of LvR fluctuation was  $0.13 \pm 0.06$  (mean  $\pm$  standard deviation) and its effect size (Cohen's *d*) was  $0.6 \pm 0.2$ . These results suggest that the firing pattern of individual DCN neurons may contribute to somatosensory discrimination.

**Keywords:** dorsal column nuclei; inter-spike interval; moving tactile stimuli; spike train; touch  
Tohoku J. Exp. Med., 2017 October, 243 (2), 115-126. © 2017 Tohoku University Medical Press

## Introduction

Dorsal column nuclei (DCN) are the first relay station for somatosensory inputs from the periphery. These neurons integrate somatosensory information and send the output to higher-order areas, such as thalamic relay nuclei, before the output is further processed in the cerebral cortex and ultimately perceived as rich and vivid somesthetic sensation. Despite the functional importance of DCN in the somatosensory neuraxis, the coding principles underlying the processing of somatosensory information in this region remain substantially unknown. In anatomical terms, one DCN neuron is thought to receive inputs from 300 different primary afferents (Jones 2000). The transmission between a single afferent and its target neuron in the DCN is quite stable, such that a single presynaptic action potential (spike) corresponds to a single postsynaptic spike (Rowe 2002). This type of transmission security has been demonstrated in the kinesthetic afferents from muscles and joints and in various types of skin afferents from hair follicles, Pacinian cor-

puscles, Merkel cells, and Ruffini endings (Rowe 2002). However, based on an analysis of miniature and saturated excitatory postsynaptic potentials (EPSPs) in the DCN, only approximately 4-8 primary afferents are likely to functionally dominate the inputs (*i.e.*, DCN neurons do more than passively relay information) (Bengtsson et al. 2013). On the other hand, human microneurography studies have demonstrated that the latency with which the brain detects these tactile features is so short that only single spikes in individual afferents can be utilized for stimulus detection (Johansson and Birznieks 2004). Thus, single spikes elicited from across a population of afferents in an ensemble must convey information important for tactile recognition. These meaningful combinations of afferent spikes occurring within a short time window are thought to determine the instantaneous firing rate of individual DCN neurons and, ultimately, their overall firing patterns. Therefore, numerical evaluation of the firing patterns (*i.e.*, analysis of spike train inter-spike intervals [ISIs]) of individual DCN neurons is important for understanding somatosensory information

Received July 10, 2017; revised and accepted October 4, 2017. Published online October 26, 2017; doi: 10.1620/tjem.243.115.

Correspondence: Takashi Toda, Ph.D., D.D.S., Division of Oral Physiology, Tohoku University Graduate School of Dentistry, 4-1 Seiryomachi, Aoba-ku, Sendai, Miyagi 980-8575, Japan.  
e-mail: ttoda@m.tohoku.ac.jp

processing.

The firing patterns of DCN neurons *in vivo* have long been of interest because these neurons often exhibit characteristic bursts or irregularity (Amassian et al. 1964; Amassian and GIBLIN 1974; Golovchinsky 1980; Pubols et al. 1989; Canedo et al. 1998; Panetsos et al. 1998; Nuñez et al. 2000; Soto et al. 2004; Sánchez et al. 2006; Witham and Baker 2011; Richardson et al. 2016). A few of these studies quantified the firing patterns based on one of two numerical metrics: the coefficient variation of ISIs (CV) (Amassian and GIBLIN 1974; Pubols et al. 1989) and the logarithmic ratio of consecutive ISIs (IR) (Richardson et al. 2016). However, these metrics, particularly the CV, are susceptible to firing rate fluctuations, and the resulting evaluations are less reliable (Shinomoto et al. 2009). Another metric, LvR, which is the local variation in ISIs compensated by the refractoriness constant, R (*i.e.*, the cross-correlation between consecutive ISIs compensated by the refractoriness constant R) was devised to overcome this disadvantage and has been applied to analysis of neurons in the cerebral cortex of conscious monkeys, including the motor-related, visual, and prefrontal areas (Shinomoto et al. 2009). However, LvR has yet to be employed for the assessment of neuronal activity in the DCN, which is the first relay station of the somatosensory system.

In the present study, we investigated a range of LvRs in DCN neurons in anesthetized rats. These results were compared with those obtained from functionally-defined cortical areas in conscious macaque monkeys (Shinomoto et al. 2009). In addition, although it is generally believed that the firing pattern of individual neurons is stable, the extent to which the LvR changed in particular neurons when the features of tactile stimuli changed was investigated. If the LvR changed significantly, the temporal firing pattern as well as the firing rate of individual DCN neurons could provide information required for somatosensory discrimination of stimulus features.

To the best of our knowledge, the present study is the first to demonstrate a range of LvR in DCN neurons. Furthermore, it was verified that a substantial proportion of the present sample exhibited significant differences in LvR when moving tactile stimuli were applied in different directions.

Some data from this study have been reported in abstract form (Toda and Shishido 2017).

## Materials and Methods

### *Neurophysiology and histology*

This study was performed in 12 female Wistar rats weighing between 259 and 317 g. All experimental procedures were approved by The Institutional Animal Care and Use Committee of the Tohoku University Environmental and Safety Committee. The rats were anesthetized with a mixture of medetomidine (0.15 mg/kg), midazolam (2 mg/kg), and butorphanol tartrate (2.5 mg/kg) via intramuscular injection. Artificial respiration was not used because tracheal cannulae interfere with the exploration of receptive fields (RFs)

around the neck. Each rat was placed in a stereotaxic apparatus that allowed easy access to the orofacial area and pectoral girdle, electrocardiography and peripheral capillary oxygen saturation (SpO<sub>2</sub>) were monitored continuously, and the body temperature was kept at 37–38°C by placing a disposable warm pad beneath the rats. Under a dissecting microscope, an occipital craniotomy was performed, the brain stem was exposed, and the dura matter was deflected to permit the penetration of a recording electrode. The penetrations were made in the range between 0.2 mm rostrally and 1.0 mm caudally to the obex, and between 0.8–1.3 mm lateral to the mid-line, and at a depth of up to 1.3 mm, which is mostly consistent with the method in a previous study on rat DCN (Sánchez et al. 2006).

Single-unit activity was recorded extracellularly in the DCN using an ordinary tungsten microelectrode (FHC; Bowdoin, ME, USA) with a final taper angle of 10–15° in the last 120 μm, epoxyite insulation, an electrode resistance of 5–7 MΩ, and a differential amplifier (WPI, Sarasota, FL, USA). The position of the recordings was visually controlled using a dissecting microscope and the neurons were searched while listening to their amplified activities over acoustic speakers (sound monitor). RFs on the body surface were identified using a hand-held paintbrush with a ferrule (3.5 mm in diameter) at the far end, while RFs of deep structures were identified using forceps. As a substantial proportion of DCN neurons exhibited no or few spontaneous discharges, the somatosensory response was carefully checked whenever the electrodes were advanced. The distinction between DCN neurons and primary afferent fibers was made based on previous observations (Towe and Jabbur 1961; Amassian et al. 1964; Sánchez et al. 2006); these studies showed that positive action potentials (spikes) and very brief negative spikes (*e.g.*, 100 μs) likely represent the activity of afferent or passing fibers. Therefore, only activities displaying monophasically negative spikes or initially negative spikes succeeded by a smaller positive phase in which the half-amplitude widths were more than 150 μs were collected.

Once a putative single neuron was identified, stimuli that sufficiently elicited maximum or near-maximum responses to obtain a greater number of spikes were determined. Data acquisition sessions for each neuron consisted of repeated stimulation trials with intervals of 1–2 s in which sustained mechanical stimuli, such as light stroking across skin RFs (moving tactile stimuli) or passive movements of forelimb joints, were made with hand-held apparatuses. The stimuli were applied with force-sensing apparatuses developed by our research group and included a modified paint brush for hair deflection and a thin plastic probe for passive movements of forelimb joints. The modified paintbrush had a handle intercalated by a plastic sheet with a strain gauge on it; the thin plastic probe was nearly rectangular in shape (60 × 9 mm) with a strain gauge attached to its middle.

Following a preliminary examination using these apparatuses, it became apparent that the stimuli could be kept constant across trials while carefully listening to spike firing through the sound monitor without sensing the force directly. Therefore, in 9 of 17 neurons (53%), either the aforementioned normal paintbrush or forceps without the strain gauge was used due to ease of handling. In most neurons responsive to hair deflection, moving tactile stimuli were applied in different directions (2–4 directions for each neuron), including the anterior-posterior, posterior-anterior, medial-lateral, and lateral-medial directions. In each direction, efforts were made to apply the moving stimuli with a velocity sufficient to elicit a maximum or near-maximum response that was determined prior to data acquisition. Single-unit activities were continuously collected at a sampling rate

of 25 kHz using 16-bit resolution (CED, Cambridge, UK) and stored on a personal computer for off-line analysis (Dell Precision T7500; Intel Xeon quad core processor with a 3.33 GHz clock speed and 4 GB memory).

At the end of the selected penetrations, electrolytic lesions were made for subsequent identification of the recording loci. Each rat was sacrificed with an overdose of pentobarbital sodium, the brain was removed, blocked, and immersed in 10% formalin; the lower brain stem was cut into serial transverse sections of 100  $\mu\text{m}$  in thickness. Each section was Nissl-stained with 0.25% cresyl violet and the electrolytic lesions were identified. Finally, the recording loci restricted to the DCN were identified based on the manipulator readings obtained during recording and histological observations.

#### Data analysis: general aspects

In the analysis of neuronal responses, single neurons were identified off-line using a template matching algorithm and subjected to principal component analyses (CED, Cambridge, UK). To ensure that the recording was made from a DCN neuron rather than fibers, the polarity and width of each spike were verified again at this stage. The spike train extent during the stimulus period in each trial was determined by the onset and offset of the strain gauge output or as distinct barrages of spikes evoked by somatosensory stimuli (described in detail later).

Next, it was estimated whether each of the recorded neurons projected to the thalamus based on previous findings in anesthetized rats (Nuñez et al. 2000). These authors reported that neurons with low spontaneous activity ( $1.9 \pm 0.48$  spikes/s) represented 74% of their sample and were identified as thalamic projection neurons based on antidromic activation by the electrical stimulation of the projection pathway (*i.e.*, medial lemniscus); the remaining 26% of neurons exhibited a high firing rate ( $27.2 \pm 5.1$  spikes/s) and were not antidromically activated. Considering these results, the present study regarded a neuron as thalamic projection neuron if its spontaneous firing rate was less than 3 spikes/s.

#### Data analysis: neuronal firing rate and firing pattern during stimuli

The data were exported to Scilab (Scilab Enterprises S.A.S, Orsay Cedex, France), which was installed on an additional personal computer (Fujitsu Esprimo WH77/S; Intel Core i7-4712MQ processor with a 2.30 GHz clock speed and 8 GB memory); all Scilab scripts used in this study were written by one of its authors (T. T.). First, the temporal fluctuation of the firing rate in each neuron was examined on a peri-stimulus time histogram (PSTH). For all neurons in the present sample, it was verified that the firing rate during the stimulus was higher than the upper confidence limit of spontaneous activity during the 1.0-s pre-stimulus period, as previously described (Abeles 1982). In cases where the force-sensing probe was not used, the stimulus onset of each trial was easy to identify because the DCN neurons investigated in the present study displayed no or low spontaneous activity. On the other hand, the stimulus offset was sometimes ambiguous and rather difficult to determine due to a gradual decrease in the firing rate. Therefore, for all cases, the time point in the post-peak period of the PSTH when the count decreased to 60% of the peak was determined and set as the practical endpoint of the spike train. The mean firing rate and firing pattern (temporal structures of the spike trains) were analyzed between the first spike barrage and this endpoint. Gross periodicity (*i.e.*, oscillation and its approximate frequency) was assessed by visually inspecting the autocorrelation

histograms of 1 ms bin-widths with 11 ms-wide sliding averages. To quantify the temporal structure of the spike trains, the LvR, which is a metric of local variation in ISIs devised by Shinomoto et al. (2009), was used:

$$LvR = \frac{3}{n-1} \sum_{i=1}^{n-1} \left( 1 - \frac{4I_i I_{i+1}}{(I_i + I_{i+1})^2} \right) \left( 1 + \frac{4R}{I_i + I_{i+1}} \right),$$

where  $I_i$  and  $I_{i+1}$  are consecutive ISIs,  $R$  is the refractoriness constant, and  $n$  is the number of ISIs. As the refractoriness constant prevents apparent regularity due to the refractory period of the spike, especially when the firing rate is high, the LvR metric can evaluate the regularity (or irregularity) of the ISI independent of fluctuations in firing rate. The refractoriness constant was set at 0.005 s, as previously described (Shinomoto et al. 2009). Fig. 1 shows three representative spike trains from the present sample and their LvRs. From A to C in Fig. 1, LvR takes higher value as the difference in consecutive ISIs becomes larger on average.

All analyses, including statistical tests, were performed using a bootstrap method with a resampling rate of 10,000, except for the evaluation of the effect size between different stimuli and to determine the regression line between the firing rate and LvR. The means of the LvR and firing rate were determined with a non-overlapping block bootstrap procedure (Carlstein 1986), which regards each stimulus trial as a discrete block. When a neuron was tested using moving stimuli in different directions, the significance of the differences among the means was assessed with the bootstrap test (two-sided,  $p < 0.025$  for both). In this analysis, the test statistic was the difference in means (*i.e.*, the observed value of the test statistic was compared with the empirical distribution of simulated ones) (Efron and Tibshirani 1993). The effect size was evaluated by Cohen's  $d$  (Cohen 1988) calculated from the mean difference (range of fluctuation) and standard deviation (SD) of the original data, not the bootstrapping sample. A bootstrap procedure was used again to compare the fluctuation ratio between the LvR and firing rate. The fluctuation ratio for both the LvR and firing rate was simply calculated as

$$Fluctuation\ Ratio = \frac{M_1 - M_2}{M_{max} - M_{min}},$$

where  $M_1$  and  $M_2$  are the means of different stimulus directions and  $M_{max}$  and  $M_{min}$  are the maximum and minimum mean values among the total sample, respectively.

A cluster observation analysis was also used to compare responses of stimulus pairs in a more intuitive manner (*i.e.*, the results from all the bootstrap replicates for the LvR and firing rate were graphically plotted on the bivariate plane). For these distributions, 95% confidence regions were determined using a principal component analysis such that, after centralization and normalization, the data were transformed to a new coordinate system of the first and second principal components. Next, the Euclidean distances between each replicate and mean on the coordinates were calculated and the replicates for which the distances were below the 95<sup>th</sup> percentile were identified and plotted over the total replicates. Finally, visual inspection was performed to determine whether the confidence regions of different stimuli overlapped in terms of either LvR or firing rate; if the confidence regions of two clusters did not overlap, the difference was regarded as significant. Theoretically, the probability that the true centers of the clusters were close to each other beyond the confi-

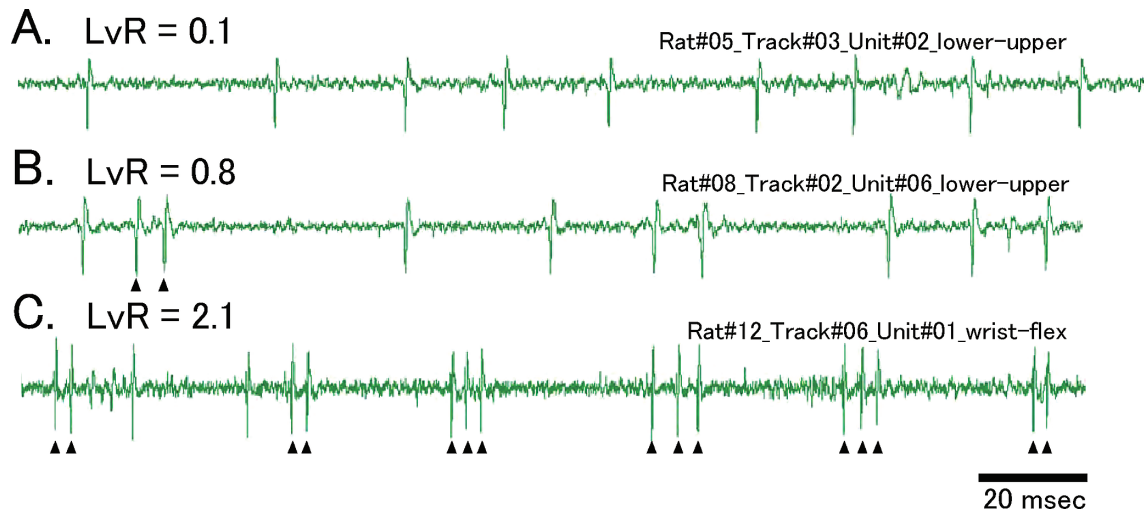


Fig. 1. Representative examples of spike trains and their local variations in inter-spike intervals (LvR).

Shown are representative examples of trains of action potentials (spikes) and their values of LvR (i.e., a reliable index of the cross-correlation between consecutive intervals of spikes compensated by the refractoriness constant, R). The refractoriness constant was set to 0.005 s (see Materials and Methods). Spike trains were extracted from the responses of three representative neurons. Values of LvR are shown as calculated from the limited spikes presented here. (A) Regular firing, (B) Nearly random firing, (C) Bursting firing. Small black arrowheads show doublet or triplet spikes that could increase LvR. The value of LvR increased as spike trains became more irregular from (A) to (C) (i.e., the differences in consecutive intervals of spikes became larger on average).

dence regions is much lower than 0.025. In terms of the size of the bootstrap replicates, resampling at 100, 1,000, and 10,000 times was attempted for some neurons. A rate of 10,000 times was chosen because the 95% confidence regions appeared as ellipse-like forms with smooth boundaries and because the consumed calculation time was tolerable (300 min at most).

#### Data analysis: regression analysis of the relationship between firing pattern and firing rate

The relationship between the LvR and the mean firing rate was also examined. First, the gradient of the regression line on the scatter plots of the original data (not the bootstrapping sample), which were centralized and normalized, was determined. Next, the significance of the gradient was tested (i.e., whether it was zero or not) according to a bootstrapping method described previously (Wu 1986). The test statistic was

$$T = \hat{\beta} / (\hat{\sigma} / \sqrt{S_{xx}}),$$

where  $\hat{\beta}$  represents the estimate of the slope of regression,  $\hat{\sigma}$  is an estimate of the standard error of the regression, and  $S_{xx}$  is the sum of squares of x values (normalized firing rate). In cases where moving stimuli in different directions were applied, the significance of the difference in the gradient between the stimulus directions was examined using a bootstrapping test modified from a permutation test described previously (Vieira and Creed 2013). The test statistic was the difference in the gradients of the original data sets.

## Results

### General aspects

In total, 61 single neurons were identified extracellularly along 21 penetrations in the DCN. All of the neurons were verified to be located within the DCN based on the

manipulator readings obtained during recording and histological observations that the electrolytic lesions of recording loci were localized to the DCN (see Materials and Methods). Excluding neurons with phasic responses, 21 of the 61 neurons were selected and their activities were stored on a personal computer. Following off-line inspection, 17 of these 21 neurons with a sufficient number of well-isolated action potentials (spikes) were subjected to numerical analysis. The neurons were recorded from the following regions in the rostrocaudal and mediolateral positions with respect to the obex: caudally at 0 mm (n = 10), 0.3 mm (n = 5), 0.4 mm (n = 1), and 0.5 mm (n = 1); laterally at 0.8 mm (n = 4), 1.0 mm (n = 9), 1.2 mm (n = 2), and 1.3 mm (n = 2). Most neurons (12 of 17, 70.6%) exhibited spontaneous activities with less than 3 spikes/s during the pre-stimulus period: they were regarded as putative thalamic projection neurons (see Materials and Method). Of the 17 neurons, 12 responded exclusively to hair deflection (hair neurons) while the remaining five responded exclusively to forelimb joint movement (deep submodality neurons). In 11 of the 12 hair neurons, moving tactile stimuli were applied in different directions: two directions (n = 7), three directions (n = 2), and four directions (n = 2), with 25 pairs of comparisons in total. Moving tactile stimuli were applied at low velocities (< 20 mm/s) throughout data acquisition because this type of stimulus tends to elicit a greater number of spikes, as reported previously (Castiglioni and Kruger 1985). For each neuron and each stimulus direction, the number of stimulus trials ranged from 26 to 135 (mean  $\pm$  SD: 67.6  $\pm$  23.6), whereas the number of collected ISIs ranged from 629 to 8,647 (mean  $\pm$  SD: 3,204  $\pm$  2,479).

Visual inspection of the autocorrelation histograms

(data not shown) indicated that about half of the neurons (9/17) displayed oscillations of activity with frequencies around the alpha band (10-20 Hz). The oscillations occurred regardless of their firing pattern (*i.e.*, regular, random, or bursts).

#### Analysis of neuronal firing pattern and firing rate

An overview of the LvR (firing pattern or temporal structure of spike train) and firing rate in each neuron is shown in Fig. 2A. As the responses to moving tactile stimuli in different directions were treated separately, the total number of samples was 34. The LvR ranged from 0.35 to 2.28 but was roughly concentrated around 1.0 and 2.0. The latter cluster with higher LvR obviously corresponded to

bursting neurons in the DCN that have been well studied; a representative spike train is shown in Fig. 1C. The firing rate also exhibited a wide range (13.6-77.8 Hz) but was concentrated around 20-50 Hz. The range of fluctuation and the extent of variance (fluctuation ratio, see Materials and Methods) for the LvR and firing rate were examined in each pair of comparisons ( $n = 25$ ) when the moving stimuli were applied in different directions. The range of fluctuation was  $0.09 \pm 0.07$  (mean  $\pm$  SD) in LvR, and  $8.93 \pm 8.90$  (mean  $\pm$  SD) in the firing rate. As speculated based on the data in Fig. 2B, the variance was much smaller for the LvR than for the firing rate (means  $\pm$  SD; LvR:  $4.5 \pm 3.8\%$  and firing rate:  $13.6 \pm 13.3\%$ ;  $p = 0.0029$ ). Here, one neuron that displayed the largest fluctuation in firing rate (asterisk

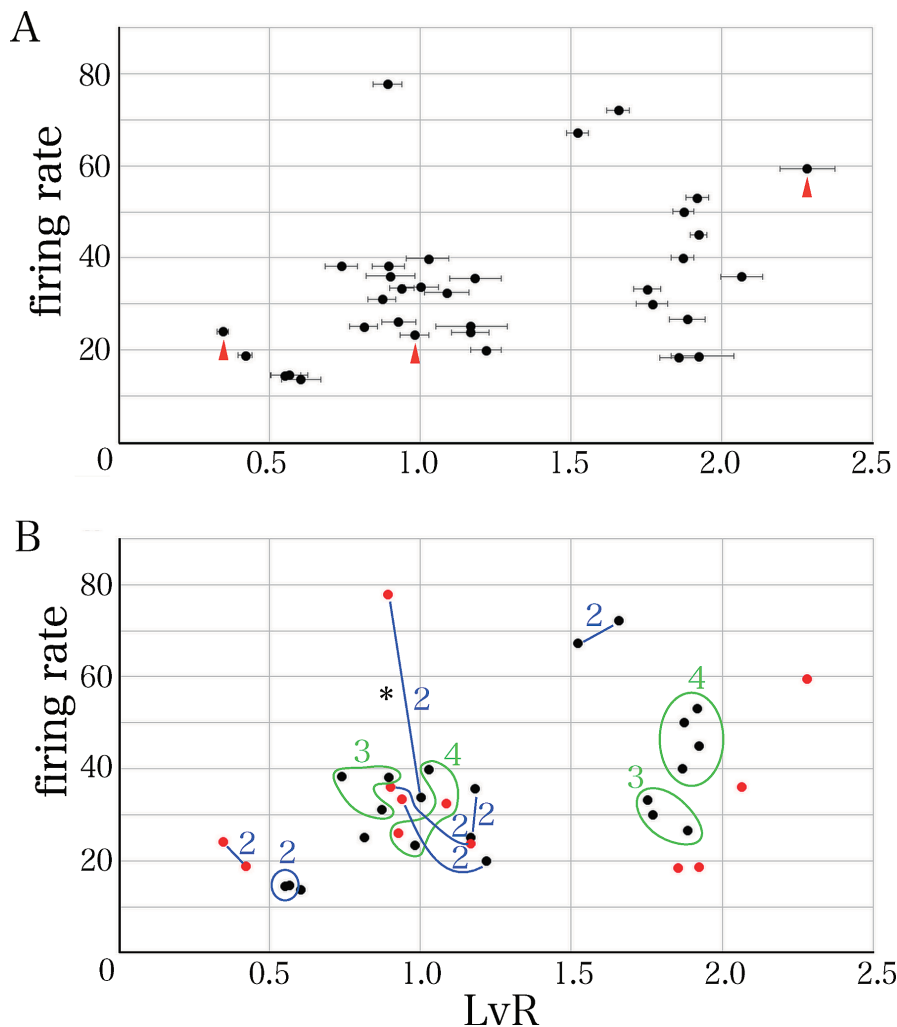


Fig. 2. Distributions of LvR and firing rate for the entire sample.

As the responses to moving tactile stimuli in different directions were treated separately, the total number of samples was 34. (A) Mean LvR and firing rate; 95% confidence interval limits are shown only for LvR for the purpose of clarity, and the three red arrowheads correspond to the representative spike trains in Fig. 1. (B) Responses of the same neuron to moving tactile stimuli in different directions categorized by the number of stimulus directions; blue and green color codes show the cases of two directions, and three or four directions, respectively. The asterisk indicates the neuron considered to be a putative outlier (see Results), which showed a prominent change in firing rate. The red dots show cases where the regression gradients were statistically significant between the LvR and firing rate, and were all negative. They were widely distributed along the LvR axis, indicating a tendency for the spike trains to be more regular with increasing firing rate regardless of the firing pattern.

in Fig. 2B) was considered to have some influence on the results. When this neuron was excluded from the analysis as a putative outlier, the significance was even greater (means  $\pm$  SD; LvR:  $4.5 \pm 3.9\%$  and firing rate:  $11.3 \pm 6.8\%$ ;  $p = 0.0002$ ).

Cases showing a significant relationship between LvR and firing rate are also shown in Fig. 2B (red dots). These 12 cases, in which the slopes of regression lines were all negative, were widely distributed along the LvR axis. That is, the regularity of ISI during neuronal firing tended to increase as the firing rate increased regardless of the firing pattern.

In Figs. 3 and 4, distributions of the 10,000 bootstrap samples (replicates) for each stimulus direction are plotted on the bivariate plane; the replicates formed a cluster (gray plots) and the 95% confidence region of each cluster (red plots) was well demarcated. In one neuron (Fig. 3), moving stimuli were applied in three directions (Fig. 3A-C). The stimulus directions corresponded to three clusters, two of

which overlapped slightly (Clusters a, b in Fig. 3D, E). On the other hand, the 95% confidence regions were entirely discrete among the three clusters (Fig. 3D). In this case, the bootstrapping statistical test showed three types of significant differences among the stimulus directions: a difference in LvR, a difference in firing rate, and differences in both. Even when using stricter criteria (*i.e.*, observation of cluster discreteness; see Materials and Methods), the same results were obtained. From these analyses, the dependence on LvR or firing rate could be estimated in a particular pair of stimulus directions. For example, in one pair (Fig. 3D; Clusters a, b), there was a significant difference in LvR but not firing rate. That is, the neuron was likely to discriminate the stimulus features of this pair based on LvR rather than firing rate. Fig. 4 shows the two other examples in which overlapping clusters were observed. In one neuron (Fig. 4A), four stimulus directions were tested and two of the six pairs of directions showed a significant difference in LvR and all six showed significant differences in the firing

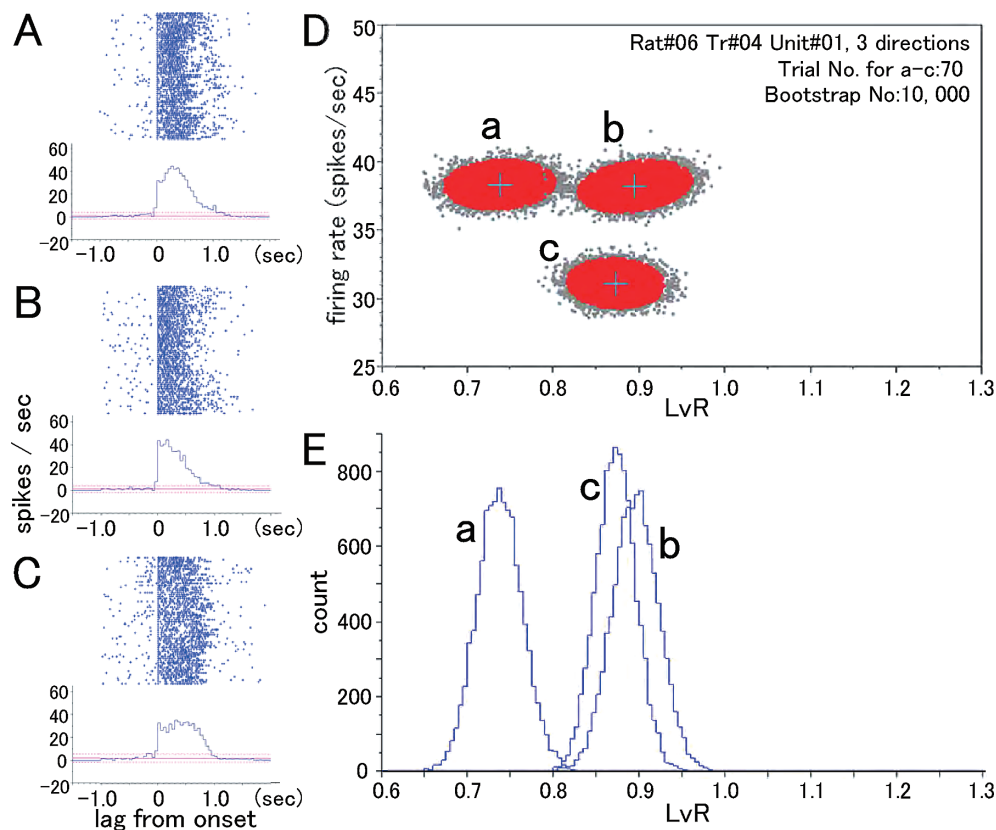


Fig. 3. Example of neuronal responses in which moving tactile stimuli were applied in three different directions.

This neuron had a receptive field (RF) on the chest and shoulder and responded to the deflection of guard hairs. (A)-(C) Raster plots of responses to stimuli in the anterior-posterior, medial-lateral, and lateral-medial directions, respectively; for each direction, 70 stimulus trials were performed. (D) 10,000 bootstrap samples (replicates) in each stimulus direction plotted on the bivariate plane of the LvR and firing rate; replicates that fell in the 95% confidence region (red) are overlaid on the total replicates (gray); cross-mark shows mean LvR and firing rate. Clusters (a)-(c) correspond to raster plots of responses (A)-(C), respectively. The confidence regions of the three clusters do not overlap. The bootstrapping statistical test revealed three types of significant difference among the stimulus directions: a difference in LvR (Clusters a-b), a difference in firing rate (Clusters b-c), and differences in both (Clusters a-c). The cluster observation analysis using much stricter criteria (see Materials and Methods) yielded the same results. (E) Histogram showing the distributions of LvR in each direction.

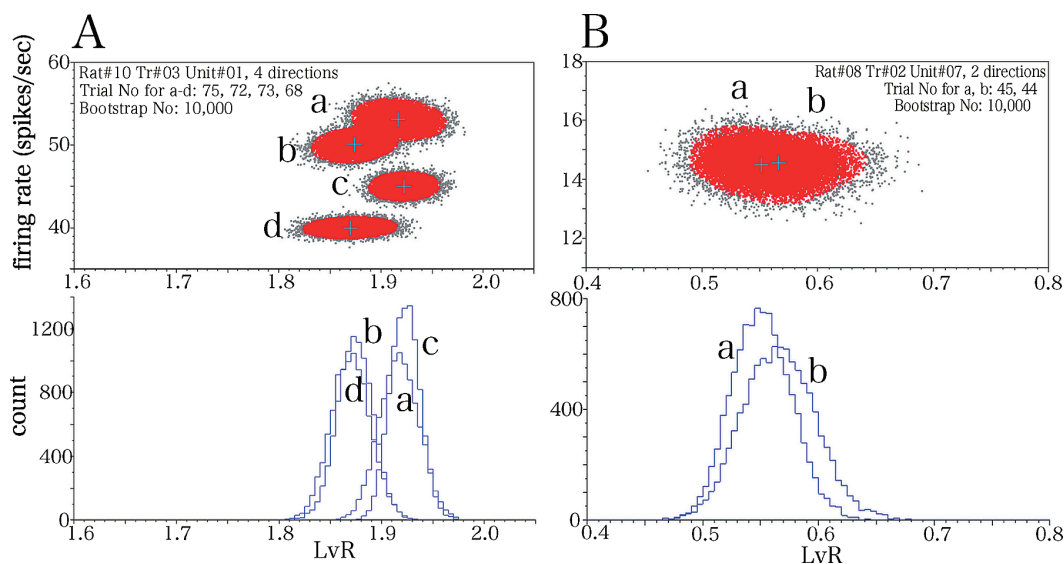


Fig. 4. Two neurons in which moving tactile stimuli were applied in different directions.

Two neurons in which moving tactile stimuli were applied in different directions, and overlapping clusters were observed. (A) This neuron had a RF on the neck and shoulder, and responded to deflection of guard hairs. Each cluster corresponds to stimulus in the (a) lateral-medial, (b) anterior-posterior, (c) posterior-anterior, and (d) medial-lateral directions. The confidence regions of the top two clusters (a) and (b) overlapped each other; bootstrapping statistical tests revealed that only the firing rate differed significantly. In the bootstrapping test, two of the six pairs of comparisons showed a significant difference in LvR and all six showed significant differences in firing rate, while in the cluster observations, none showed significant difference in terms of LvR, whereas five of the six pairs showed significant differences in firing rate. (B) This neuron had RF on the neck and responded to deflection of guard hairs. Left (a) and right (b) clusters correspond to the lateral-medial and anterior-posterior directions, respectively, and show a large degree of overlap; bootstrapping statistical test and cluster observations revealed that the LvR and firing rate did not differ significantly. Other conventions are as in Fig. 3D, E.

rate in the bootstrapping test. In the cluster observation, none showed significance in the LvR whereas five of the six pairs showed significance in the firing rate. That is, as far as could be determined in this case, the neuron was likely to code the stimulus features based on firing rate rather than LvR. In another neuron tested with two stimulus directions (Fig. 4B), the two clusters showed a large degree of overlap and there were no significant differences in terms of either LvR or firing rate in the bootstrapping test and cluster observations; the neuron did not seem to be suitable to discriminate this particular stimulus pair. Dependency on LvR or firing rate was examined in all 25 pairs (Table 1). The proportions of pairs that showed significant differences in firing rate, LvR, and both were 88%, 56%, and 52%, respectively. In the cluster observation using much stricter criteria, the proportions of pairs that showed significant differences in firing rate, LvR, and both were 72%, 24%, and 16%, respectively. Although both analysis methods revealed a dependency on firing rate rather than LvR in total, a substantial proportion of neurons showed a significant difference in LvR between stimulus directions. The range of fluctuation in the pairs that showed a significant difference in the bootstrapping test was  $0.13 \pm 0.06$  (mean  $\pm$  SD) in LvR and  $9.99 \pm 8.97$  (mean  $\pm$  SD) in the firing rate. Their effect size (*i.e.*, Cohen's *d*) of the firing rate (mean  $\pm$  SD;  $1.2 \pm 0.6$ ) was larger than that of the LvR (mean  $\pm$  SD;  $0.6 \pm 0.2$ ).

#### Regression analysis of the relationship between LvR and firing rate

In some cases, the bootstrap replicates were obliquely distributed in the bivariate plane (see Figs. 3D and 4A), which might reflect the possible correlation between LvR and firing rate. To examine this quantitatively and statistically, we calculated the regression gradients in each cluster of centralized and normalized data. Fig. 5A, B show two examples of neurons in which the regression gradients were significant; the gradient determined based on the original data is shown on the left and that determined based on the 10,000 bootstrap replicates is shown on the right. Although the gradients of the original data and the bootstrap replicates were similar in most cases, as shown here, the original data were used in the analyses, including statistical tests. A summary of the regression analyses (Fig. 5C) showed that the slopes ranged widely from  $-0.79$  to  $+0.25$ . The total number of samples was 34, because the responses to moving tactile stimuli in different directions were treated separately. Of these, 35.3% (12 of 34 cases) showed significant relationships in which the slopes were all negative (red lines) whereas the remaining 22 did not show a significant relationship (gray lines). The significant negative gradients revealed a tendency for the spike trains to be more regular as the firing rate increased. Evaluations to determine whether the slopes of each neuron exhibited significant changes when the stimuli were applied in different direc-

Table 1. Proportion of stimulus pairs that exhibited differences in LvR or firing rate with changes in the direction of moving tactile stimuli.

		LvR		Sum
		Significant	Non-significant	
Firing rate	Significant	13 (52%)*	9 (36%)	22 (88%)
		4 (16%)**	14 (56%)	18 (72%)
	Non-significant	1 (4%)	2 (8%)	3 (12%)
		2 (8%)	5 (20%)	7 (28%)
Sum		14 (56%)	11 (44%)	25 (100%)
		6 (24%)	19 (76%)	25 (100%)

\*The upper rows show the results of the bootstrapping statistical test (*i.e.*, the number of pairs and its proportion to all 25 pairs).

\*\*The lower rows show the results of the cluster observation (*i.e.*, the number of pairs and its proportion to all 25 pairs).

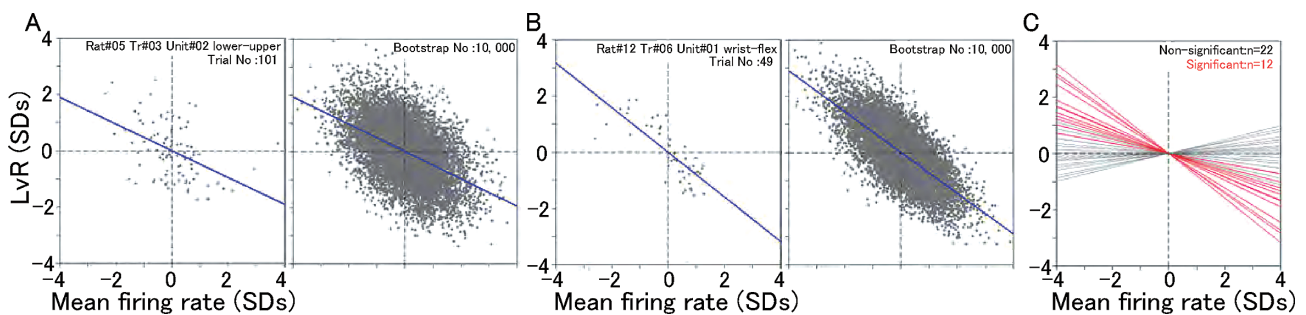


Fig. 5. Regression analysis of the relationship between LvR and firing rate.

Analyses were performed in each neuron or in each stimulus direction when more than two directions were tested ( $n = 34$ ). Note that the X-Y axes have been exchanged so that the LvR is plotted against firing rate; both axes represent deviation of the values from the means and are normalized to the standard deviation (SD). (A) and (B) Two examples of neurons in which the regression gradients were statistically significant and negative. The gradients were determined based on the original data (left) and the 10,000 bootstrap replicates (right); in the original data, each dot represents the result of each stimulus trial, while in the bootstrap replicates each dot represents each bootstrap replicate. The gradients of the original data and those of the bootstrap replicates were similar [in (A):  $-0.48$  vs.  $-0.49$  and in (B):  $-0.79$  vs.  $-0.72$ ] as in most cases in the present study. The gradients of the original data were used in the analyses including statistical tests. For (A), the means of the firing rate and LvR were 24.1 Hz and 0.35 (regular firing pattern), respectively; for (B), 59.4 Hz and 2.28 (bursting firing pattern), respectively; the regularity of intervals of spikes tended to increase as the firing rate increased regardless of the firing pattern, as shown in Fig. 2B. (C) Summary of the regression lines. Of the total of 34 cases, 12 showed statistical significance and all had a negative relationship (red lines).

tions revealed that, of the 25 pairs of comparisons, only one pair exhibited a significant difference. Thus, the relationship between the LvR and the firing rate was stable for individual neurons regardless of the stimulus direction of moving tactile stimuli, as far as could be determined in these cases.

## Discussion

### Methodology

A mixture of medetomidine, midazolam, and butorph-

anol, which is a method recommended by the guidelines of our institute, was used to induce anesthesia and analgesia in the present study. A search of the literature did not reveal any previous neurophysiological studies investigating the DCN that used these anesthetics but all neurons in the present sample responded very well to the mechanical stimuli. In fact, some of these neurons were bursting neurons (Figs. 1C and 2) that have been often featured in DCN studies as mentioned in the Introduction. A substantial proportion of neurons displayed oscillations with frequencies around the



alpha band (10-20 Hz), which is consistent with the findings of previous studies (Panetsos et al. 1998; Nuñez and Buño 1999; Nuñez et al. 2000; Reboresda et al. 2003; Sánchez et al. 2006; Richardson et al. 2016); such an oscillation has been speculated to reinforce the spatiotemporal summation of information at the target nucleus (Nuñez et al. 2000; Sánchez et al. 2006). Furthermore, it has been reported that the activities of DCN neurons do not differ under different types of anesthetics, including urethane, pentobarbital, and a mixture of ketamine and xylazine (Nuñez et al. 2000). Thus, it can be speculated that the activities of DCN neurons are less susceptible to differences based on different anesthetics and that the present results are comparable to those of previous DCN studies using different anesthetics.

As reliable LvR analyses require a substantial number of action potentials (spikes) per trial, the present sample was inevitably limited to neurons that displayed a vigorous tonic response regardless of whether they were hair neurons or deep submodality neurons responsive specifically to forelimb joint movements. The mechanical stimuli were applied with a hand-held force-sensing probe, simple brush, or forceps; thus, it is possible that the manual stimulation and the responses to this stimulation might have fluctuated from trial to trial. To account for this issue and to minimize its effects as much as possible, care was taken to keep the stimuli constant so that maximum or near-maximum responses could be elicited while listening to the sound monitor. In addition, when the moving tactile stimuli were applied, they were applied at low velocities so that a greater number of spikes could be recorded, stable responses could be obtained across trials, and a sufficient number of spikes could be obtained overall. Another concern with the manual stimulation was that the originally phasic responses could apparently become tonic following repetitive stimulation due to physiological tremors in the hand of the experimenter. However, this possibility was ruled out because phasic responses were observed in hair neurons and deep submodality neurons using the present stimulation method.

Most neurons in the present sample (12 of 17, 70.6%) were considered to be thalamic projection neurons because they displayed spontaneous activity with a low firing rate (< 3 spikes/s, see Materials and Methods). This may have been because all 17 neurons were recorded from the DCN region near the rostrocaudal level of the obex, which is a “slab region” of the rat DCN that possesses the greatest concentration of thalamic projection neurons (Tan and Lieberman 1978; Massopust et al. 1985; Mantle-St. John and Tracey 1987; Willis and Coggeshall 1991; Sánchez et al. 2006). Despite such a biased proportion of the putative projecting neurons and the small sample size ( $n = 17$ ) in the present study, neurons with various types of firing patterns were encountered and analyzed (Fig. 2A) and neurons with LvR that changed significantly in response to different stimulus directions were observed (Figs. 2B and 3, Table 1). Therefore, the size and composition of the present sample

were likely sufficient to achieve the stated experimental objectives.

#### *Neuronal firing pattern and firing rate*

The neuronal firing pattern (temporal structure of spike trains) and firing rate are thought to be important for the accurate representation of somatosensory information. To reliably quantify firing patterns, the LvR metric was adopted (Shinomoto et al. 2009). This metric evaluates the cross-correlation between consecutive ISIs and can be used to evaluate the regularity (or irregularity) of ISIs independent of fluctuations in firing rate. LvR has been used to show that firing patterns differ among functionally-defined cortical areas in conscious macaque monkeys, including frontal association areas, visual areas, and motor-related areas (Shinomoto et al. 2009). It was also recently reported that this tendency is preserved across different animal species (Mochizuki et al. 2016). Furthermore, using LvR, it was shown that the firing patterns of particular neurons exhibit significant changes in the monkey prefrontal cortex depending on the epochs of the behavioral task (Sakamoto et al. 2013). In that study, a transient increase in LvR (range of fluctuation: c.a. 0.1-0.2) was considered to represent a less stable state intercalated between stable states of the neural circuits based on an empirical analysis and the results from neural network models. Using this reliable LvR metric, we quantified the firing patterns of DCN neurons and alterations in these patterns in the present study. To our knowledge, there have been no modeling studies involving LvR analysis in the DCN. The present study might provide basic data to construct DCN models and their related ascending somatosensory pathway.

Initial studies demonstrated variability in the firing patterns of DCN neurons. In particular, the bursting neuron has long been a subject of concern in these relay nuclei, as mentioned in the Introduction, Results, and earlier in this section. Similarly, the present study found that the LvR ranged widely from 0.35 to 2.28 but was concentrated roughly around 1.0 and 2.0 (Figs. 1 and 2); the concentration of higher LvR corresponded to bursting neurons. This pattern of LvR distribution in DCN neurons is similar to that observed in the visual cortex and even to that seen in the parietal association area, as reported by the original study using LvR (Shinomoto et al. 2009). Based in part on their findings, these authors proposed that firing irregularity increases in ascending sensory pathways as these signals move further toward higher-order cortical areas and then decreases in cortical motor areas. This pattern likely does not occur in the somatosensory system, based on previous findings regarding bursting neurons and the present results from the DCN. The present study also showed that the fluctuation ratio and effect size for LvR were lower than those of the firing rate, which supports the generally accepted idea that each neuron has a characteristic firing pattern.

### *Alteration of firing pattern by stimulus features*

The idea that the firing patterns of DCN neurons might contribute to the discrimination of stimulus features initially appeared in a pioneering study (Amassian and GIBLIN 1974). A more recent study demonstrated that single spikes elicited across a population of afferents in an ensemble must code tactile features (Johansson and Birznieks 2004). These meaningful combinations of afferent spikes within a short time window are considered to determine the instantaneous firing rate of DCN neurons and, ultimately, their overall firing patterns. When the stimulus features change, the firing pattern changes due to subtle differences in the relative timing of spikes in individual tactile afferents. Indeed, some previous studies have reported that the activities of DCN neurons change depending on stimulus features (Castiglioni and Kruger 1985; Jörntell et al. 2014); however, there are no numerical evaluations of the firing patterns (temporal structure of spike trains) of individual neurons in these studies. In a rat study, controlled air-jet stimuli administered in different directions were applied to the hairy skin and directional differences in the neuronal responses were detected by visual inspection (Castiglioni and Kruger 1985).

Another recent study systematically tested haptic features, such as contact initiation and cessation, slip, and rolling contact, in glabrous cat skin (Jörntell et al. 2014) and clearly demonstrated that each haptic feature was distinctively represented by a combination of DCN neuronal activities. The authors analyzed 10 different periods between 15 and 150 ms after stimulus onset and showed that a linear classification of haptic features was evident even at 30 ms; the linear classification was based on the number of spikes in short time windows (bins) of 5–10 ms. This firing time course revealed by such a binning approach that discretize time might be reflected as a firing pattern (temporal structure of spike trains) of individual DCN neurons. For example, in Fig. 3D, the mean firing rate was 38 Hz for Clusters a and b, and the LvRs were 0.74 and 0.90, respectively. When the LvR was changed from 0.74 to 0.90 and the bin-width was 5 ms, the probability at which one spike moved to a neighboring bin was 26.8%, which was quite high. The present findings showed that firing patterns, as assessed by LvR, differed significantly in 56% of the pairs of comparisons (Table 1). Even when using much stricter criteria (the cluster observation), the proportion of pairs with significant difference was still 24% (Table 1). Considering that significant changes in firing rate (Table 1) were found in up to 88% of the pairs (72% in the cluster observation) and that the fluctuation ratio and effect size were higher in the firing rate than in LvR, the firing pattern might additively contribute to the detection of stimulus features. Our present results cannot exclude the possibility that discrimination of the features might depend on the recruitment of distinct neuronal populations consisting of neurons with particular firing patterns (e.g., regular or bursting).

In addition to the extrinsic inputs via primary afferents, another possible source of influence on firing patterns might be neural circuits within the DCN. This brain region has a substantial neural network consisting of inhibitory interneurons that release  $\gamma$ -aminobutyric acid, glycine, or both (Popratiloff et al. 1996; Soto et al. 2004), projection neurons (Tan and Lieberman 1978), and their recurrent collaterals projecting back to the DCN (Davidson and Smith 1972; Nuñez et al. 2000; Aguilar et al. 2002; Sánchez et al. 2006). Thus, the change in LvR by stimulus direction reported in the present study might reflect alterations in information processing within these local neural circuits of the DCN. In addition, intrinsic membrane properties, such as the composition and distribution of ion channels, of individual DCN neurons might influence LvR, particularly in bursting neurons. Indeed, bursting activities can be generated by microiontophoresis of glutamate into the DCN (Galindo et al. 1968) and antidromically by electrical stimulation of the thalamus or lemniscal pathway (Rowinski et al. 1985; Sánchez et al. 2006), and even in cultured DCN neurons without neural connections (Reboreda et al. 2003). However, in the present study, some bursty neurons had LvR that exhibited a significant change between stimulus directions (Fig. 4A). In such cases, the changes in extrinsic afferent inputs and the state of DCN circuits might contribute to the modification of firing patterns rather than membrane properties.

### *Setting of refractoriness constant in LvR and relation of LvR and firing rate*

In the original LvR study (Shinomoto et al. 2009), the optimal value of the refractoriness constant,  $R$ , was determined empirically to be 5 ms, which was able to discriminate firing patterns among cerebral cortical neurons most effectively. In this study, it was also noted that “the value was comparable to the known refractory period for neuronal firing.” Generally, however, the full post-spike recovery cycle that may influence the generation of subsequent spikes, including the relative refractory period and super- and sub-normal periods, may be much longer (McIntyre et al. 2002; Bucher and Goillard 2011) and may be different from neuron to neuron. Therefore, it may be reasonable to adjust the  $R$  depending on the properties of the neuronal population studied, and more importantly, on the experimental purposes. Indeed, the  $R$  was set to 11 ms in a subsequent study of the monkey prefrontal cortex (Sakamoto et al. 2013). Nonetheless, in the present study, we set  $R$  to 5 ms according to the original study for ease of comparison of the LvR between the present and the original study by Shinomoto et al. (2009). A study on rat DCN showed that a single spike of DCN neurons is followed by a depolarizing after-potential, if any, and an after-hyperpolarization lasting tens of milliseconds (Nuñez and Buño 1999). In this study, no differences were observed in the time course of the spike or its recovery cycle between putative projection neurons and interneurons; therefore, there was little effect of the

composition of both neuronal types in the present sample. In a study using a neonatal rat brain stem preparation (Deuchars et al. 2000), the spike duration of DCN neurons measured from the start of the rising phase of the spike to the start of the after-hyperpolarization was c.a. 8 ms on average. Thus, the R in the present study (5 ms) seemed to include the absolute and relative refractory periods, and possibly parts of the super- or sub-normal period.

In the original LvR study on the cerebral cortex (Shinomoto et al. 2009), these authors demonstrated that the LvR can detect the firing patterns of individual neurons with stronger invariance for firing rate fluctuation than the other five metrics (*i.e.*, there is no correlation between LvR and firing rate). Nonetheless, in the present study, the slope of the regression line in 12 of 34 cases (35.3%) was statistically significant and all were negative (Fig. 5C). It is probable that the bivariate correlation may reflect firing characteristics that are specific to individual neurons such that the regularity of firing tends to increase as the firing rate increases (negative slope). It is also possible that the R (5 ms) in the present study was too short to compensate for the refractory effect in DCN neurons that displayed maximum or near-maximum responses with shorter ISIs. Indeed, it was validated in our sample that the regression slope became less steep when a larger R was used (data not shown). However, the duration of the post-spike recovery cycle of DCN neurons (Nuñez and Buño 1999) is comparable to that of pyramidal neurons in the prefrontal cortex (Dégenétais et al. 2002), although a study using a neonatal rat brainstem preparation reported a prominent after-hyperpolarization lasting for more than 250 ms (Deuchars et al. 2000). Taken together, it is not likely that the R (5 ms) in the present study is too short.

#### Future prospects

The temporal analysis of neural activities could conceivably lead to future improvements in brain-machine-brain interfaces (BMBI), which have been developed to restore normal sensorimotor function to body parts. This technology requires appropriate electrical microstimulation in the central nervous system to give rise to artificial tactile sensations (O'Doherty et al. 2011; Medina et al. 2012). Neurophysiological studies of DCN neurons, as well as somatosensory neurons in the cerebral cortex, will play an important role in determining the optimal electrical stimulus conditions for BMBI.

As the present investigation was limited to putative maximum or near-maximum responses for each neuron or each stimulus direction, future studies will be necessary to examine how the LvR is altered in a wider range of firing rates using more strictly controlled stimulus conditions. It also remains to be clarified whether the LvR or the relationship between the LvR and firing rate differs between projection and non-projection neurons or between skin and deep submodality neurons.

#### Acknowledgments

We sincerely thank Professor Tsuboi A. for his careful reading of the draft version of this manuscript in Japanese (part of a master's thesis by S. Shishido at Tohoku University) and his constructive comments. The English in this document has been checked by at least two professional editors, both native speakers of English. For a certificate, please see: <http://www.textcheck.com/certificate/a1LhJN>

#### Conflicts of Interest

The authors declare no conflicts of interest.

#### References

- Abeles, M. (1982) Quantification, smoothing, and confidence limits for single-units' histograms. *J. Neurosci. Methods*, **5**, 317-325.
- Aguilar, J., Soto, C., Rivadulla, C. & Canedo, A. (2002) The lemniscal-cuneate recurrent excitation is suppressed by strychnine and enhanced by GABA<sub>A</sub> antagonists in the anaesthetized cat. *Eur. J. Neurosci.*, **16**, 1697-1704.
- Amassian, V.E. & Glibin, D. (1974) Periodic components in steady-state activity of cuneate neurones and their possible role in sensory coding. *J. Physiol.*, **243**, 353-385.
- Amassian, V.E., Macy, J. Jr., Waller, H.J., Leader, H.S. & Swift, M. (1964) Transformation of afferent activity at the cuneate nucleus. In *Information processing in the nervous system*, edited by Gerard, R.W. & Duff, J.W., Excerpta Medica Foundation, Amsterdam, Netherlands, pp. 235-255.
- Bengtsson, F., Brasselet, R., Johansson, R.S., Arleo, A. & Jörntell, H. (2013) Integration of sensory quanta in cuneate nucleus neurons *in vivo*. *PLoS One*, **8**, e56630.
- Bucher, D. & Goaillard, J.M. (2011) Beyond faithful conduction: short-term dynamics, neuromodulation, and long-term regulation of spike propagation in the axon. *Prog. Neurobiol.*, **94**, 307-346.
- Canedo, A., Martinez, L. & Mariño, J. (1998) Tonic and bursting activity in the cuneate nucleus of the chloralose-anesthetized cat. *Neuroscience*, **84**, 603-617.
- Carlstein, E. (1986) The use of subsamples values for estimating the variance of a general statistic from a stationary sequence. *Ann. Statist.*, **14**, 1171-1179.
- Castiglioni, A.J. & Kruger, L. (1985) Excitation of dorsal column nucleus neurons by air-jet moving across the skin. *Brain Res.*, **346**, 348-352.
- Cohen, J. (1988) *Statistical Power Analysis for the Behavioral Sciences*, 2nd ed., Lawrence Erlbaum Associates, Hillsdale, NJ.
- Davidson, N. & Smith, C.A. (1972) A recurrent collateral pathway for presynaptic inhibition in the rat cuneate nucleus. *Brain Res.*, **44**, 63-71.
- Dégenétais, E., Thierry, A.M., Glowinski, J. & Gioanni, Y. (2002) Electrophysiological properties of pyramidal neurons in the rat prefrontal cortex: an *in vivo* intracellular recording study. *Cereb. Cortex*, **12**, 1-16.
- Deuchars, S.A., Trippenbach, T. & Spyer, K.M. (2000) Dorsal column nuclei neurons recorded in a brain stem-spinal cord preparation: characteristics and their responses to dorsal root stimulation. *J. Neurophysiol.*, **84**, 1361-1368.
- Efron, B. & Tibshirani, R.J. (1993) Hypothesis testing with the bootstrap. In *An introduction to the bootstrap*, Springer Science + Business Media, Dordrecht, Netherlands, pp. 220-236.
- Galindo, A., Krnjević, K. & Schwartz, S. (1968) Patterns of firing in cuneate neurones and some effects of Flaxedil. *Exp. Brain Res.*, **5**, 87-101.
- Golovchinsky, V. (1980) Patterns of responses of neurons in

- cuneate nucleus to controlled mechanical stimulation of cutaneous velocity receptors in the cat. *J. Neurophysiol.*, **43**, 1673-1699.
- Johansson, R.S. & Birznieks, I. (2004) First spikes in ensembles of human tactile afferents code complex spatial fingertip events. *Nat. Neurosci.*, **7**, 170-177.
- Jones, E.G. (2000) Cortical and subcortical contributions to activity-dependent plasticity in primate somatosensory cortex. *Annu. Rev. Neurosci.*, **23**, 1-37.
- Jörntell, H., Bengtsson, F., Geborek, P., Spanne, A., Terekhov, A.V. & Hayward, V. (2014) Segregation of tactile input features in neurons of the cuneate nucleus. *Neuron*, **83**, 1444-1452.
- Mantle-St. John, L.A. & Tracey, D.J. (1987) Somatosensory nuclei in the brain stem of the rat: independent projections to the thalamus and cerebellum. *J. Comp. Neurol.*, **255**, 259-271.
- Massopust, L.C., Hauge, D.H., Ferneding, J.C., Doubek, W.G. & Taylor, J.J. (1985) Projection systems and terminal localization of dorsal column afferents: an autoradiographic and horseradish peroxidase study in the rat. *J. Comp. Neurol.*, **237**, 533-544.
- McIntyre, C.C., Richardson, A.G. & Grill, W.M. (2002) Modeling the excitability of mammalian nerve fibers: influence of afterpotentials on the recovery cycle. *J. Neurophysiol.*, **87**, 995-1006.
- Medina, L.E., Lebedev, M.A., O'Doherty, J.E. & Nicolelis, M.A. (2012) Stochastic facilitation of artificial tactile sensation in primates. *J. Neurosci.*, **32**, 14271-14275.
- Mochizuki, Y., Onaga, T., Shimazaki, H., Shimokawa, T., Tsubo, Y., Kimura, R., Saiki, A., Sakai, Y., Isomura, Y., Fujisawa, S., Shibata, K., Hirai, D., Furuta, T., Kaneko, T., Takahashi, S., et al. (2016) Similarity in neuronal firing regimes across mammalian species. *J. Neurosci.*, **36**, 5736-5747.
- Núñez, A. & Buño, W. (1999) *In vitro* electrophysiological properties of rat dorsal column nuclei neurons. *Eur. J. Neurosci.*, **11**, 1865-1876.
- Núñez, A., Panetsos, F. & Avendaño, C. (2000) Rhythmic neuronal interactions and synchronization in the rat dorsal column nuclei. *Neuroscience*, **100**, 599-609.
- O'Doherty, J.E., Lebedev, M.A., Ifft, P.J., Zhuang, K.Z., Shokur, S., Bleuler, H. & Nicolelis, M.A. (2011) Active tactile exploration using a brain-machine-brain interface. *Nature*, **479**, 228-231.
- Panetsos, F., Núñez, A. & Avendaño, C. (1998) Sensory information processing in the dorsal column nuclei by neuronal oscillators. *Neuroscience*, **84**, 635-639.
- Popratiloff, A., Valtchanoff, J.G., Rustioni, A. & Weinberg, R.J. (1996) Colocalization of GABA and glycine in the rat dorsal column nuclei. *Brain Res.*, **706**, 308-312.
- Pubols, B.H. Jr., Haring, J.H. & Rowinski, M.J. (1989) Patterns of resting discharge in neurons of the raccoon main cuneate nucleus. *J. Neurophysiol.*, **61**, 1131-1141.
- Reboreda, A., Sánchez, E., Romero, M. & Lamas, J.A. (2003) Intrinsic spontaneous activity and subthreshold oscillations in neurones of the rat dorsal column nuclei in culture. *J. Physiol.*, **551**, 191-205.
- Richardson, A.G., Weigand, P.K., Sritharan, S.Y. & Lucas, T.H. (2016) A chronic neural interface to the macaque dorsal column nuclei. *J. Neurophysiol.*, **115**, 2255-2264.
- Rowe, M.J. (2002) Synaptic transmission between single tactile and kinaesthetic sensory nerve fibers and their central target neurones. *Behav. Brain Res.*, **135**, 197-212.
- Rowinski, M.J., Haring, J.H. & Pubols, B.H. Jr. (1985) Response properties of raccoon cuneothalamic neurons. *Somatosens. Res.*, **2**, 263-280.
- Sakamoto, K., Katori, Y., Saito, N., Yoshida, S., Aihara, K. & Mushiaki, H. (2013) Increased firing irregularity as an emergent property of neural-state transition in monkey prefrontal cortex. *PLoS One*, **8**, e80906.
- Sánchez, E., Reboreda, A., Romero, M. & Lamas, J.A. (2006) Spontaneous bursting and rhythmic activity in the cuneate nucleus of anaesthetized rats. *Neuroscience*, **141**, 487-500.
- Shinomoto, S., Kim, H., Shimokawa, T., Matsuno, N., Funahashi, S., Shima, K., Fujita, I., Tamura, H., Doi, T., Kawano, K., Inaba, N., Fukushima, K., Kurkin, S., Kurata, K., Taira, M., et al. (2009) Relating neuronal firing patterns to functional differentiation of cerebral cortex. *PLoS Comput. Biol.*, **5**, e1000433.
- Soto, C., Aguilar, J., Martín-Cora, F., Rivadulla, C. & Canedo, A. (2004) Intracuneate mechanisms underlying primary afferent cutaneous processing in anaesthetized cats. *Eur. J. Neurosci.*, **19**, 3006-3016.
- Tan, C.K. & Lieberman, A.R. (1978) Identification of thalamic projection cells in the rat cuneate nucleus: a light and electron microscopic study using horseradish peroxidase. *Neurosci. Lett.*, **10**, 19-22.
- Toda, T. & Shishido, S. (2017) Spiking patterns of somatosensory neurons in the first relay nuclei in the rat medulla: their sensitivity to directions of moving tactile stimuli. *J. Oral Biosci. Suppl.*, **2017**, 457.
- Towe, A.L. & Jabbur, S.J. (1961) Cortical inhibition of neurons in dorsal column nuclei of cat. *J. Neurophysiol.*, **24**, 488-498.
- Vieira, V.M.N.C.S. & Creed, J. (2013) Estimating significances of differences between slopes: a new methodology and software. *Comput. Ecol. and Softw.*, **3**, 44-52.
- Willis, W.D. Jr. & Coggeshall, R.E. (1991) Sensory pathways in the dorsal funiculus. In *Sensory mechanisms of the spinal cord*, 2nd ed., Plenum Press, New York, NY, pp. 245-306.
- Witham, C.L. & Baker, S.N. (2011) Modulation and transmission of peripheral inputs in monkey cuneate and external cuneate nuclei. *J. Neurophysiol.*, **106**, 2764-2775.
- Wu, C.F.J. (1986) Jackknife, bootstrap and other resampling methods in regression analysis (with discussion). *Ann. Statist.*, **14**, 1261-1350.